




Soil Erosion Vulnerability Assessment in the Eco-Sensitive Himalayan Region Using Modeling Approach

Shiba Zahoor¹ · Akhlaq Amin Wani¹  · Aasif Ali Gatoo¹ · M. A. Islam¹ · Shah Murtaza¹ · T. H. Masoodi¹ · P. K. Joshi²

Received: 3 January 2023 / Accepted: 16 April 2024 / Published online: 24 May 2024
© Indian Society of Remote Sensing 2024

Abstract

Soil loss due to erosion has a huge impact on worldwide economy and environment. The Himalayan region is extremely vulnerable to erosion due to rugged terrain, erratic precipitation and excessive anthropogenic pressures. This study attempts to assess the spatial distribution of soil loss for managing soil disintegration rates in the western Himalayas using a GIS modeling approach. Factors affecting soil erosion were assessed and mapped using primary data from the field and secondary data. Map layers were developed for each identified factors and modeled using weighted overlay analysis. The rainfall-runoff erosivity, soil erodibility, topographic, cover management and support parameters varied around 361.75 MJ mm/ha/h/yr, (0.024–0.051) t ha h/ha/MJ/mm, 0–585.372, 0–1 and 0–1 respectively. The yearly soil disintegration rate varied between 0 and 6098.44 t ha/yr. The maximum area (137,165.30 ha) of the district's total area (146,295.142 ha) was under the less vulnerable class and the minimum (259.92 ha) was under the severely vulnerable category. The findings reported 70.24% of the area was under the less vulnerable class, followed by extremely vulnerable (10.48%) > highly vulnerable (7.40%) > severely vulnerable (7.19%) > moderately vulnerable (4.69%). The maximum (810 t/ha) and minimum (15 t/ha) mean soil loss was found under severely vulnerable and less vulnerable categories. The findings will provide site specific data regarding soil loss and vulnerability for effective management of soils in the eco-sensitive region.

Keywords Soil loss · Modeling · RUSLE · GIS · Himalayas

Introduction

Forest areas are getting changed over into different land-use frameworks in the Himalayan states of India, bringing about severe soil disintegration (Sharma et al., 2007). Soil loss influences land sustainability, productivity and rural livelihoods as it lessens land productivity and exacerbates food insecurity and poverty (Erkossa et al., 2015). As per FAO and ITPS (2015), the average soil disintegration rate is around 12–15 t/ha/yr, suggesting a loss of 0.90–0.951 mm of top soil annually. The aimless utilization of this natural resource combined with expanded human exercises

like deforestation, land clearance, ploughing and absence of management has prompted its degradation, echoing the attention of the organizers, specialists, farmers and overall population (Panagos et al., 2015; Sharma & Chaudhary, 2007). Estimates show that soil disintegration is responsible for roughly 85 per cent of land loss worldwide, diminishing crop productivity by around 17 per cent, impacting soil fertility at first and bringing about land renunciation in the long run (Singh & Panda, 2017). In India, approximately five billion tonnes of soil loss happen every year (Saroha, 2017); rivers wash away 29% of eroded soil into the ocean and 10% to the repositories leading to sediment deposition, with soil loss being more common in the Western Ghats and Himalayan region (Pandey et al., 2017; Singh et al., 1992). Compared to other countries, India's soil disintegration reports show that 29.32% of the country's total area is persevering through land degradation (Ministry of Agriculture & Farmers Welfare, 2020). Subsequently, to keep up the current degree of soil productivity and fulfil the needs of the future,

✉ Akhlaq Amin Wani
akhlaqwani@gmail.com; akhlaqwani@yahoo.co.in

¹ Division of Natural Resource Management, Faculty of Forestry, Sher-e-Kashmir University of Agricultural Sciences and Technology of Kashmir, Benhama, Ganderbal, J&K 191201, India

² School of Environmental Sciences, Jawaharlal Nehru University, New Delhi 110067, India

expanding accentuation is being placed on soil characterization, precise mapping, and soil interpretation.

To determine the soil loss impact on the worldwide economy and environment, quantitative appraisals of soil disintegration at various scales, viz. micro, meso, and macro scales, are essential (Alexakis et al., 2013). In previous investigations, multiple methodologies and procedures for quantifying soil loss have been documented (Prasannakumar et al., 2011). A wide assortment of strategies, including statistical models, process-based models, empirical models and physical models, have been used by numerous specialists to foresee soil disintegration around the world (Dimotta, 2019). Multiple investigations have anticipated the soil loss rate by integrating the Revised Universal Soil Loss Equation (RUSLE) and Geographical Information System (GIS) (Ostovari et al., 2017; Uddin et al., 2018). RUSLE is a basic model for evaluating potential soil loss, wherein yearly soil disintegration rates are determined precisely (Beskow et al., 2009). Advancements in remote sensing, climatic datasets and earth observations information are effective variables for erosion modeling (Alewell et al., 2019). The primary bit of leeway in satellite data in soil disintegration studies is its capacity to represent occasional fluctuation of vegetative cover and landscape alterations and furnish appropriate high-resolution data to study soil disintegration at the neighbourhood or territorial scale (Gianinetto et al., 2019).

The majestic Himalayas are dealing with a catchment scale disintegration issue, which produces a tremendous amount of water and dregs in streams that pass through this region, transporting a large amount of residue (Dar et al., 2014). Ongoing assessments show that almost 39 per cent of the Indian Himalayas have a soil disintegration potential rate of around 40.01 Mg/ha/yr (Mandal & Sharda, 2011). The north western part of the Himalayas faces accelerated soil disintegration because of escalated rates of forest degradation (Wani et al., 2017, 2021), cultivation on steep slants and escalated deforestation (Das et al., 1981). The majority of the Himalayan parts that represent the lower Himalayas are the most delicate biological systems due to their precarious slant, heavy downpours and unstable soil, making it vital to concentrate on its delicacy. In this context, the current examination aims to assess the vulnerability of soils to disintegration using RUSLE and GIS. The present study's findings will locate hotspot areas of soil disintegration, assist in strategic policy making for limiting the soil loss hazard and plan exercises to control soil loss and fill a gap in soil erosion data of a specific region. Additionally, the outcomes will act as reference information for researchers, scientists, government and other concerned organizations working on soil disintegration.

Materials and Methods

Study Area

The current investigation was conducted in the middle part of north western Himalayas, situated on geographical coordinates of 34° 08' 0" N 74° 35' 0" E–34° 28' 0" N 75°30' 0" E at an average elevation of 1618.9 m MSL, covering district Ganderbal (J&K, India) (Fig. 1).

The region witnesses yearly precipitation of 694.4 mm, whereas minimum and maximum temperature range between –3.98 and 16.61 °C and 9.84–30.43 °C, respectively (Anonymous, 2014). The present investigation region was chosen because of the area's higher percentage (almost 70%) under hills (Anonymous, 2011), increased agricultural frameworks, and landscape and terrain diversity, making the region more prone to soil disintegration. The major Land use land cover (LULC) types of the region include forest, agriculture, wetland, forest scrub, waterbody, trees outside the forest, built up, wasteland, grassland and snow. Three major soil types viz. loamy soils, karewa soils, and underdeveloped mountainous soils, are witnessed in the region (Raza et al., 1978).

Description of Data Sources

The climatic and terrain factors were obtained from WorldClim/nearby meteorological stations and USGS's SRTM DEM (90 m resolution). Landsat 8 OLI digital data (year-2018) obtained from USGS was used to evaluate vegetation parameters in the study area. The erodibility variable was estimated using the FAO-UNESCO world soil map and lab analysis of 84 soil samples based on soil organic carbon, soil texture, soil permeability, and structure.

RUSLE (Revised Universal Soil Loss Equation) Model

In the present study, RUSLE framed by Wischmeier and Smith (1965), was applied to determine yearly averages of soil erosion rates. It quantifies the impact of rainfall, soil texture, topography, surface runoff and vegetation on soil disintegration as evaluated by Wischmeier and Smith's (1978) equation:

$$A = R \times K \times L \times S \times C \times P$$

where A is the yearly rate of soil loss (t/ha/yr), K stands for erodibility of soil (t ha h/ha/MJ/mm), R stands for rainfall-runoff erosivity (MJ mm/ha/h/yr); L represents slope length, S stands for slope gradient, C is crop management factor, and P is management practice factor.

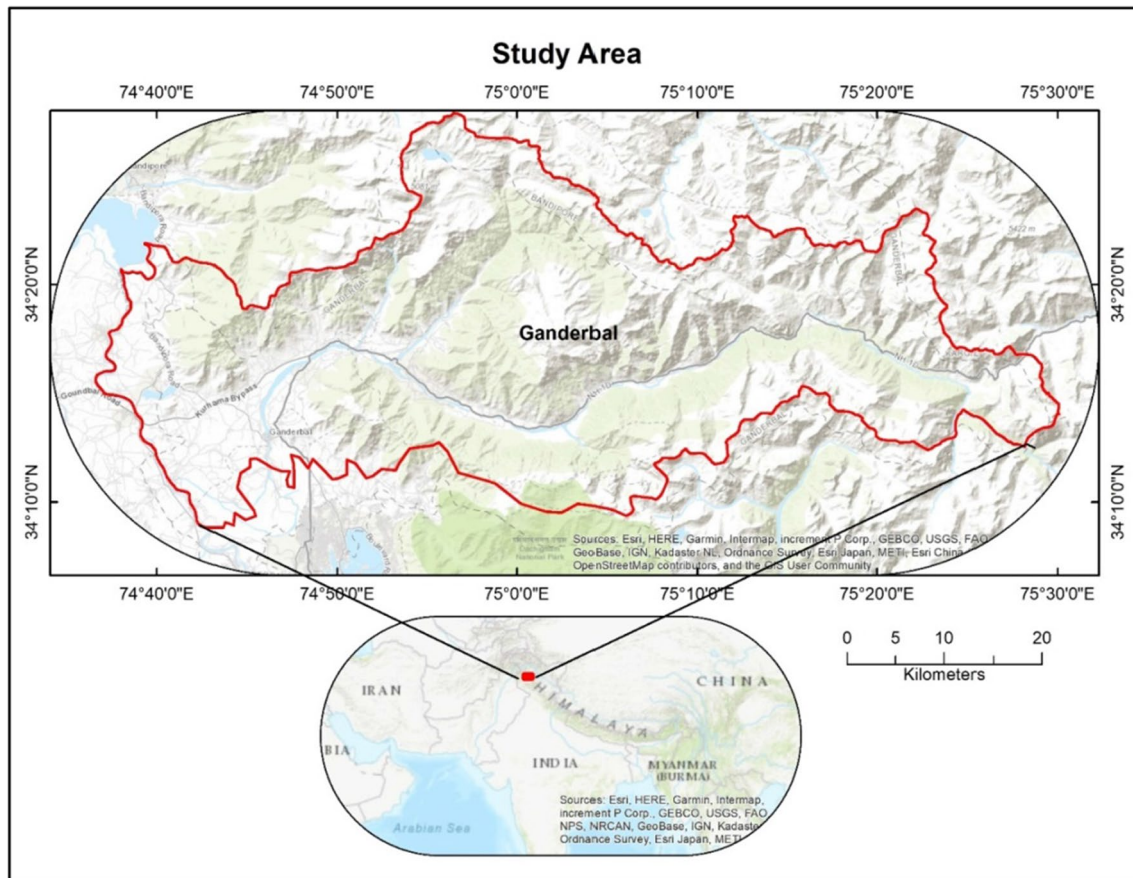


Fig. 1 Map showing the study area location

Rainfall Runoff Erosivity Factor (R)

It is a function of intensity, volume, precipitation length and results from the raindrop's kinetic energy and thirty-minute most incredible rainfall intensity (Wischmeier & Smith, 1978). Due to a deficiency of a sufficient high-resolution rainfall database obtained from the adjoining rainfall stations including Srinagar and Gulmarg, the historical rainfall dataset of WorldClim for 50 years (1950–2000) was employed to determine the average yearly precipitation. R-factor was calculated and validated using the equations given by Choudhury and Nayak (2003) and Babu et al. (2004).

$$R = 79 + 0.363 P_x \text{ (} P_x \text{ is average yearly precipitation in millimeters)}$$

$$R = 81.5 + 0.380 P_a \text{ (} P_a \text{ average yearly precipitation in millimeters)}$$

Soil Erodibility Factor (K)

It expresses the soil's vulnerability, sediment transportability, amount and rate of overflow. It varies from 0 (low

susceptibility) to 1 (high vulnerability) (Farhan & Nawaiseh, 2015). In RUSLE, the soil map attributes consist of soil texture (% sand, % clay and % silt) of various soil groups (Foster et al., 2003), % soil organic matter (Govindarajan, 1978), p (soil permeability code) (Renard et al., 1997) and s (soil structure code) (Brady & Weil, 2000). In the present study, we procured the required credentials from the FAO soil map and through a detailed field survey of different soil types of the region, followed by their subsequent collection and analysis in the lab. K variable was computed using Wischmeier et al. (1971) and Wischmeier and Smith's (1978) equations:

$$K = \frac{2.1 \times 10^{-4} (12 - OM) M^{1.14} + 3.25(s - 2) + 2.5(p - 3)}{759.4}$$

where K is soil erodibility parameter expressed in t ha h/ha/MJ/mm, OM stands for organic matter in %, p represents the permeability of soil, s gives the structural code of soil, and M is a fraction of particles computed as:

$$M = (\text{per cent silt} + \text{per cent very fine sand}) \times (100 - \text{per cent clay})$$

$$K = 27.66 \times M^{1.14} \times 10^{-8} \times (12 - A) + 0.0043 \times (B - 2) + 0.0033 \times (C - 3)$$

where M = per cent silt + per cent very fine sand \times (100 - per cent clay), A is per cent organic matter, C represents soil permeability code, B gives the structural code of soil.

Topographic Factor (LS)

The topographic factor is the predicted proportion of soil erosion in the present situation to soil loss in an area with a “standard” slant length (22.1 m) and slant steepness (9%). It is a significant component in deciding soil loss since the gravity force affects the overflow (Zhang et al., 2013). For calculating the LS factor, SRTM DEM of 90 m resolution was procured and re-projected. Flow direction map was prepared using DEM and used as input to generate a flow accumulation map. Accordingly, the slope map was prepared from the flow accumulation map. The L and S parameter was determined by using the given equation (Amsalu et al., 2007):

$$LS = \text{power}(\text{Flow accumulation}) \times \frac{\text{resolution}}{22.1, 0.4} \times \text{power}\left(\text{Sin} \frac{\text{slope} \times 0.01745}{0.09, 1.4}\right) \times 1.4 \quad (6)$$

Crop Management Factor (C)

According to Wischmeier and Smith (1978), the C factor is the proportion of soil disintegration for a given land cover to soil disintegration under cultivated continuous fallow. The map of land use land cover was made using a satellite image of Landsat 8 OLI. Based on a reconnaissance survey and researchers’ knowledge, ten LULC practices were identified, i.e. agriculture, built up, forest, forest scrub, grassland, snow, TOF, waterbody, wetland, and wasteland in the investigation territory. C factor values proportionate to LULC types were derived based on already available literature (Chadli, 2016; Fenta et al., 2016; Gupta & Kumar, 2017; Rawat et al., 2016; Zonunsanga, 2016) and knowledge of project area gathered during field survey.

Support Management Factor (P)

Renard et al. (1997) defines the P variable as the soil disintegration ratio from a specific conservation activity to up and down slant farming. Contouring, strip cropping, and terracing are agricultural management strategies that reduce runoff erosion (Ganasri & Ramesh, 2015). The P factor values were allocated based on data acquired during the site visit and previously published research (Arekhi

et al., 2012; Chadli, 2016; Ganasri & Ramesh, 2015; Zonunsanga, 2016).

Results

R Factor

The precipitation values for the referenced period ranged from 309 to 1274 mm, with a mean yearly precipitation of 778.93 mm (Fig. 2d). The R factor for the whole district, as obtained by using linear equations, remained uniform (361.75 MJ mm/ha/h/yr).

K Factor

In the present study, three soil groups, viz. Be79-2a (Eutric Cambisols medium textured, level to gentle undulating, GL (Glacial) and I-B-U (Lithosols, Cambisol and Rankers) were present, with I-B-U being the most dominant (Fig. 2c). In terms of topography, the soil unit of Be79-2a, GL and B-U represented flat, glacial and mountainous topography, respectively. As evident from the Table 1, the highest value of soil organic carbon was observed in the soil group of Be79-2a (1.07%) whereas the remaining two soil groups i.e. GL and I-B-U announced similar values of all the observed soil parameters. The soils of the study area were sandy clay loam (I-B-U and GL) and loam (Be79-2a) in texture (Fig. 2c). As quite evident from the Table 1, use of the two independent equations of K factor (Wischmeier & Smith, 1978; Wischmeier et al., 1971) produced same K values. From the K factor map, it can be seen that the value of the K factor fluctuated between 0.024 and 0.051 t ha h/ha/MJ/mm signifying low and high values of K respectively (Table 1). The low relief areas, dominated by the Be79-2a soil group, witnessed a low value (0.024 t ha h/ha/MJ/mm) of erodibility factor than other parts of the locale occupied by I-B-U and GL soils (Fig. 2e).

LS Factor

The SRTM derived DEM map showed that the study area’s elevation ranged between 1563 and 5196 m AMSL (Fig. 2b). From the slope map, it is clear that the slope of the area under investigation varied from 0 to 47 degrees (Fig. 2a). The figure shows that most of the study area had high LS factor, and the regions with gentle slants had low LS factors, coded in grey and black color, respectively. From the analysis, it was observed that the value of the topographic factor increased as the flow accumulation and slope expanded. The

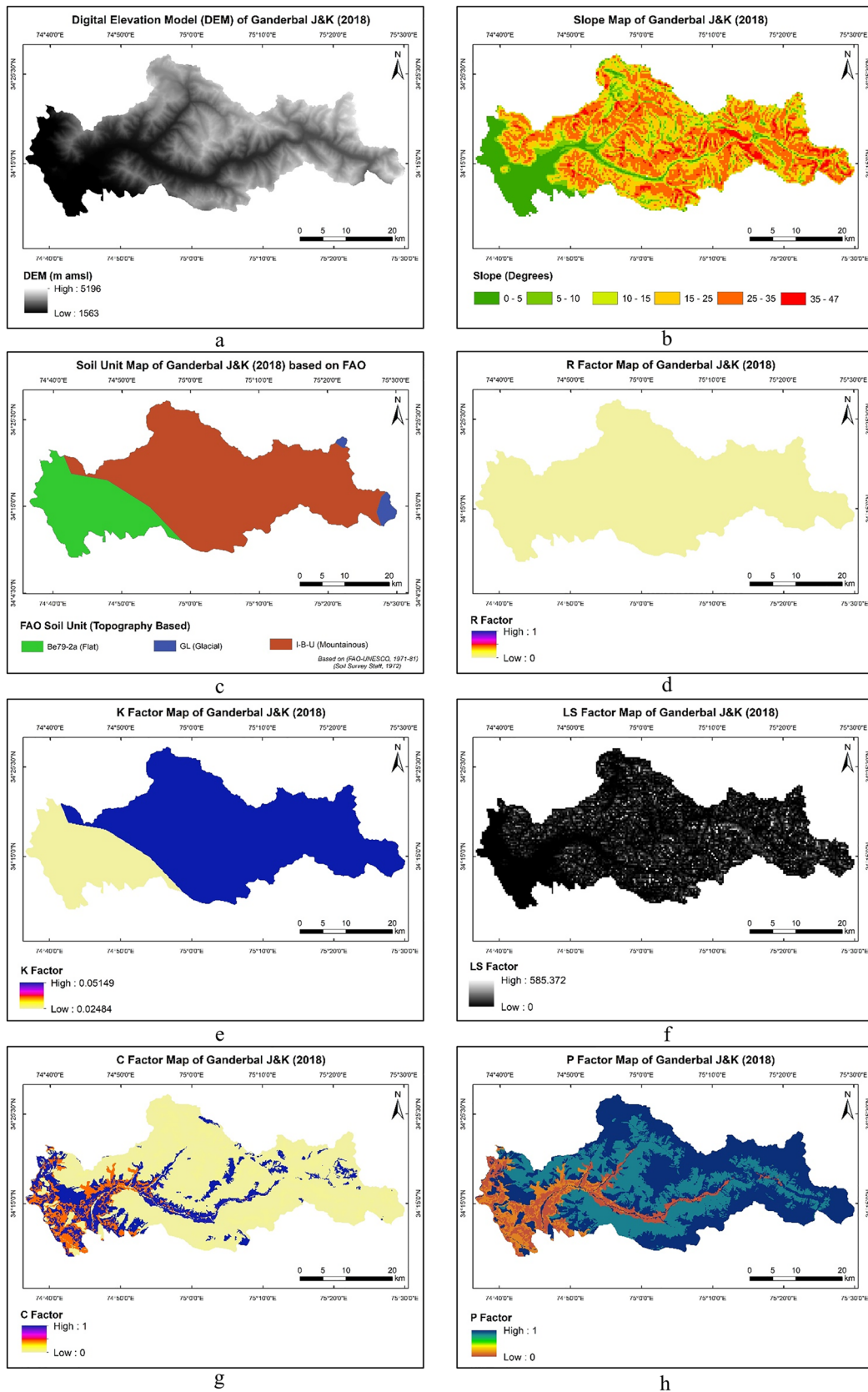


Fig. 2 a Slope map b Digital Elevation Model (DEM) c Soil unit map d R factor map e K factor map f LS factor map g C factor map h P factor map

Table 1 K factor of the major soil types in district Ganderbal

Soil unit	Soil type	Top Soil Sand (%)	Top Soil (Silt) %	Top Soil (Clay) %	Soil textural class	Organic Carbon (%)	M	Structure code	Permeability code	K factor (Wischmeier et al., 1971)	K factor (Wischmeier & Smith, 1978)
I-B-U	Lithosols, Cambisol and Rankers	58.9	16.2	24.9	Sandy clay loam	0.97	4439.59	3	4	0.05149	0.05145
Be79-2a	Eutric Cambisols medium textured, level to gentle undulating	36.4	37.2	26.4	Loam	1.07	2716.24	2	3	0.02484	0.02484
GL	Glacier	58.9	16.2	24.9	Sandy clay loam	0.97	4439.59	3	4	0.05149	0.05145

Table 2 C and P factor values of various land use land cover categories

Lulc classes	C factor	P factor
Agriculture	0.42	0.2
Built up	1	0
Forest	0.003	0.8
Forest scrub	0.3	0.9
Grassland	0.3	0.9
Snow	0	1
TOF	0.35	0.3
Waterbody	0	1
Wetland	0.3	0.9
Wasteland	1	1

low LS-factor value is mainly distributed along the gentle slope areas with low elevation whereas the very high values mainly lie in the mountainous areas having steep terrain and ridge lines.

C Factor

The C factor values were found to range from 0 to 1, where lower C values represented the areas with vegetative cover, and the higher values represented the areas with no vegetation (Table 2; Fig. 2g). The C value of various LULC categories are presented in Table 2.

P Factor

The outcomes demonstrate that snow-covered areas, waterbody and wastelands with no support practices had a higher *P*-value of 1 (Table 2; Fig. 2h). In contrast, built-up areas with minimal soil erosion had a value of 0. Due to the presence of conservation support practice (terracing) which protected the soil from erosion, the TOF practices and agriculture were assigned a value of 0.3 and 0.2, respectively (Table 2). The forest, forest scrub, grassland and wetland were assigned values close to 1 due to the absence of man-made conservation practices but the presence of vegetative cover in these land uses. As shown in (Fig. 2h), the north western portion of the study area had low *P* values whereas the middle part and upper parts had moderate and high values of *P* factor, respectively.

Annual Soil Loss (t/ha/yr)

The present study results displayed yearly soil loss of the target area in the order (0–6098.44) t/ha/yr (Fig. 3). The spatial distribution of the amount of soil loss in the study area reveals that the maximum area of the district was less susceptible to erosion with low soil loss value whereas

moderate and high erosion areas were found to be scattered in the final soil loss map.

Soil Erosion Vulnerability

To assess soil erosion severity, soil vulnerability was categorized on the basis on least, highest values and spatial soil loss as less vulnerable, moderately vulnerable, highly vulnerable, extremely vulnerable and severely vulnerable with soil loss values of (0–30) t/ha/yr, (30–60) t/ha/yr, (60–90) t/ha/yr, (90–120) t/ha/yr, (120–6100) t/ha/yr respectively. From the Fig. 4, it can be deduced that the maximum portion of the study area coded in cyan color falls under less vulnerability class (0–30) t/ha/yr with certain areas severely vulnerable to erosion which require special attention to prevent further degradation of this valuable asset. The mean soil loss under less vulnerable, moderately vulnerable, highly vulnerable, extremely vulnerable and severely vulnerable categories was 15 t/ha, 45 t/ha, 75 t/ha, 105 t/ha and 810 t/ha respectively whereas the total soil loss in the aforementioned categories was found to be around 2,057,479.50 t, 137,434.98 t, 216,874.35 t, 307,035.60 t and 210,538.70 t respectively

(Table 3). From the outcomes of the current examination, it was evident that about 70.24% of soil loss occurred under the less vulnerable class, followed by the extremely vulnerable class (10.48%) whereas only 4.69% of soil loss was witnessed in the moderately vulnerable category (Table 3). For protecting the areas from soil erosion before they reach to irreversible soil degradation, the various soil vulnerability classes were prioritized as 1st (severely vulnerable), 2nd (extremely vulnerable), 3rd (highly vulnerable), 4th (moderately vulnerable) and 5th (less vulnerable), thereby clearly depicting that severely vulnerable areas require more attention in order to prevent further loss of this value resource (Table 3).

Discussion

R Factor

The method used in the present study provides us a method to calculate the R factor using average annual rainfall. This method has also been used by several researchers in the past (Belayneh et al., 2019; Haregeweyn et al., 2017;

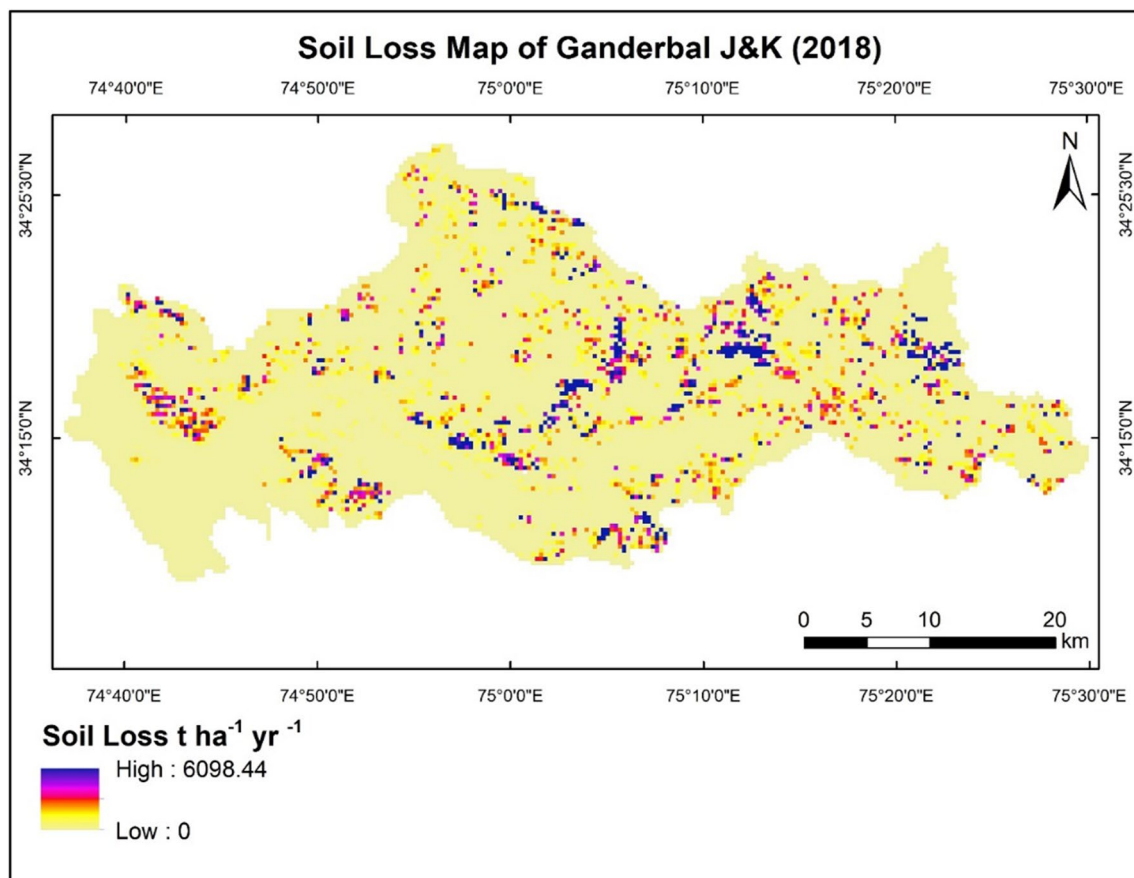


Fig. 3 Soil loss map of Ganderbal J&K (2018)

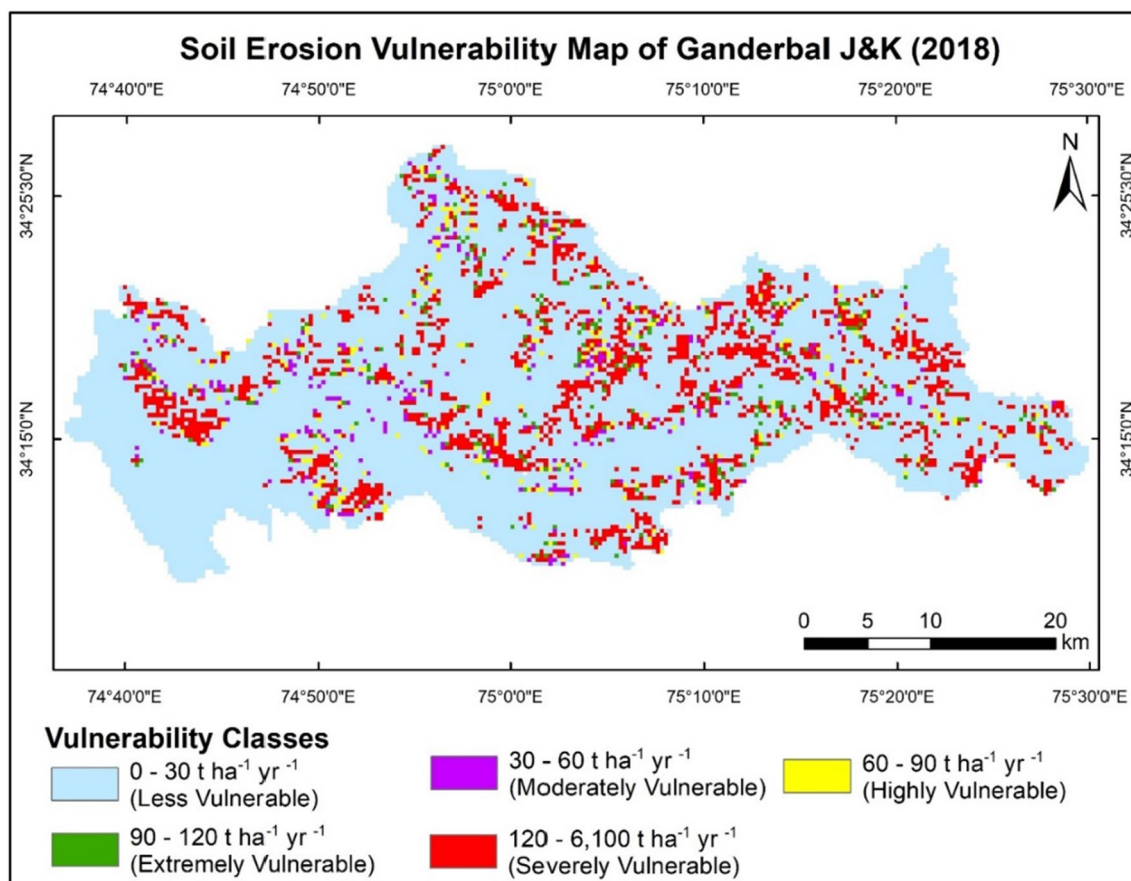


Fig. 4 Soil erosion vulnerability map of Ganderbal J&K (2018)

Table 3 Categories of soil vulnerability class, area, magnitude and proportion of each category

Soil loss (t/ha/yr)	Vulnerability classes	Area (ha)	Mean soil loss (t/ha)	Total soil loss (t)	% Soil loss	Priority class for conservation
0–30	Less vulnerable	137,165.30	15	2,057,479.50	70.24	5th
30–60	Moderately vulnerable	3054.11	45	137,434.98	4.69	4th
60–90	Highly vulnerable	2891.66	75	216,874.35	7.40	3rd
90–120	Extremely vulnerable	2924.15	105	307,035.60	10.48	2nd
120–6100	Severely vulnerable	259.92	810	210,538.70	7.19	1st
Total		146,295.142		2,929,363.141	100	

Islam et al., 2024; Kidane et al., 2019; Panditharathne et al., 2019; Shoumik et al., 2023; Thapa, 2020; Yesuph & Dagne, 2019). The noticed R factor esteems of the present study are in line with the outcomes of Panditharathne et al. (2019), who found the R factor to range between 269.70 and 454.07 MJ mm/ha/h/yr in the river basin of Kalu Ganga, Sri Lanka. Maqsoom et al. (2020) recorded the R factor between 197.345 and 349.769 MJ mm/ha/h/yr with high values in the southwestern part of Chitral district, Pakistan. R factor is influenced by slant steepness,

duration, rate and pattern of rainfall and the quantity and velocity of the subsequent overflow (Farhan & Nawaiseh, 2015). The various management practices for reducing the precipitation impact and sediment loss can be framed based on obtained R factor values (Panditharathne et al., 2019). The present study’s rainfall erosivity values are lower compared to the worldwide average (2000 MJ mm/ha/h/yr) (Borrelli et al., 2013). According to Meusburger et al. (2012) soil disintegration rate is highly receptive to precipitation. The current research region’s R factor

is much lower than that of Kidane et al. (2019) for the Western Ghats (500 and 1179.475) MJ mm/ha/h/yr and Amah et al. (2020) for South eastern part of Nigeria (5023.83–5069.51) MJ mm/ha/h/yr. The referenced studies' comparatively higher R factor values can be ascribed to differences in terrain and climatic variables. The values reported by Imajjane and Belfoul (2020) for the Beni Mohand Watershed of Morocco (35.65 and 44.56) MJ mm/ha/h/yr and Farhan and Nawaiseh (2015) for Wadi Kerak watershed, southern Jordan (54.3–227.12) MJ mm/ha/h/yr are on lower side of present study due to decreased rate of yearly precipitation in these areas. On comparing the R factor values of the present study with the reported studies, it is clear that the examination region experienced moderate mean annual rainfall, thereby making the area moderately inclined to soil disintegration.

K Factor

It determines the susceptibility of soil to disintegration, silt movability, rate and measure of overflow. Bahrami et al. (2005) consider it a rigid component to determine, demanding significant assets and time for a field inventory. In the present study, three dominant soil groups, viz. Be79-2a, GL and I-B-U are present, with I-B-U being the most dominant. It is a well-known fact that soils having lower than 3.5% OM are more vulnerable to erosion (Evans, 1980; Kumar & Kushwaha, 2013). OM (organic matter) lowers the vulnerability of soil by producing the elements that decrease soil's detachment and enhance filtration, reducing run-off and erosion (Goy, 2015). The results indicate that soil groups (I-B-U and GL) were more inclined to soil erosion due to the presence of comparatively less quantity of organic carbon (0.97%) in them. Soils with high silt content are particularly vulnerable to getting eroded, while clayey soils are the least susceptible (Brady & Weil, 2012). The soils of the study area were sandy clay loam (I-B-U and GL) and loam (Be79-2a) in texture, with soil group GL having more proportion of sand and silt, making it highly prone to disintegration. Olaniya et al. (2020) argues that soil erodibility decreases as silt content in the soil decreases, regardless of the amount of clay and sand. In the present study, the soil groups' viz. I-B-U and GL are more prone to erosion than the Be79-2a soil group. The proper explanation for this could be the presence of good soil structure (fine granular) and moderate permeability in the case of Be79-2a, whereas fair soil structure (coarse granular) and slow to average permeability in I-B-U and GL. The higher the soil erodibility values higher the chances of soil getting eroded (Ganai, 2014). The low relief areas, dominated by the Be79-2a soil group, witnessed a low value (0.024 t ha h/ha/MJ/mm) of erodibility factor than other parts of the locale occupied by I-B-U and GL soils, due to a higher percentage of organic carbon, better

soil structure and moderate permeability of Be79-2a soils bringing about the reduced vulnerability of soil to erosion. Amah et al. (2020) for Edda-Afikpo Mesas, South Eastern Nigeria and Jazouli et al. (2017) for the Ikkour watershed, Morocco reported soil erodibility ranging from (0.027 to 0.30) t ha h/ha/MJ/mm and (0.05 to 0.41) t ha h/ha/MJ/mm; respectively. Both are neck to neck with estimations of the current investigation (0.024–0.051) t ha h/ha/MJ/mm. The soil erodibility values reported by Bera (2017) of Muhuri (river basin) Tripura, India (0.34–0.36) t ha h/ha/MJ/mm and Barman et al. (2020) for Mizoram's river basin (Tuiriial) (0.51–0.66) t ha h/ha/MJ/mm are on the higher side of the current study. As announced by the mentioned studies, the significant variation in the K factor was due to differences in edaphic, climatic factors and soil texture and other soil parameters.

LS Factor

In the present study, the slope map outlined gradient progressions over distance; each pixel was color-coded depending on the landscape's steepness. Compared to terrain units on gentle slopes, steep slope terrain units often have significantly higher erosion rates since these units are made of weak rock, have poor vegetation cover, and are prone to landslides (Farhan et al., 2014). Other than this, water flows faster down steeper slopes, raising surface stress and allowing more quantity of silt to be transported (Haile & Fetene, 2012). In the present study, an increase in the topographic factor (LS factor) was observed when flow accumulation and the slope increased. Imajjane and Belfoul (2020), contend that soil erosion is more common on moderate slopes due to soft rocks, creating weak soils that are more vulnerable to decay, while hard rock protects slopes and resistant floors from erosion on steep slopes. The findings of the current investigation are in line with the results of Wang et al. (2019) for Nanling National Nature Reserve, South China, who obtained an LS factor in the range of 0–612.105. However, much higher values (0–92,774) were reported by Ganasri and Ramesh (2015) in southwestern India's basin (Nethravathi). Comparatively lower values than the current investigation were reported by Amah et al. (2020) for Edda-Afikpo Mesas, South Eastern Nigeria (2.5–59.5) and Das et al. (2020) for Kameng watershed, Arunachal Pradesh (0–39.57). According to Tamiru and Wagari (2021), the slope significantly impacts the soil loss rate, with slope values of more than 11% more susceptible to erosion. According to Wischmeier and Smith (1978), among the topographical factors, the impact of the S factor on soil loss is significantly more than that of the L factor because as the slope steepness rises, so does soil erosion due to increased velocity and erosion. The outcomes of the present study indicate that the low LS factor is along with the gentle slope areas with low elevation.

In contrast, the exceptionally high values mainly lie in steep terrain and ridgelines in mountainous regions.

C Factor

This variable addresses the impact of plants, biomass and disturbing soil exercises on soil loss (Manjulavani et al., 2016). It is likely the most significant element in RUSLE because it addresses factors that are easy to handle to avoid or minimize soil erosion (McCool et al., 1995). The presence of vegetation cover is vital as the roots of plants enhance the shear and cohesion strength among soil particles, along these lines, forestalling repetitive soil drooping, mudflows and shallow avalanches (Farhan & Nawaiseh, 2015). Densely vegetated regions with low human impedances are connected with most minimal C values (< 0.2), thereby pointing towards increased protection of soil against erosion (Bouhadab et al., 2018). Studies by Labriere et al. (2015) affirmed that even if a leaf layer is present, the absence of understory vegetation will bring about expanded soil loss. Although the leaf layer initially collects raindrops, over time, it becomes too heavy and much larger drops are released. In the current examination, the built-up and wetland with no vegetative cover were doled out a value of 1. Built-up areas minimize erosion by concretizing the soil and increasing erosion by disrupting the soil. Farhan and Nawaiseh (2015) announced that values of crop management in southern Jordan differed somewhat between 0 and 0.91, with a value of 0.05–0.10 (for scattered forest areas) and 0.5 (for barren land and open rangeland). Agricultural lands help fix soil disintegration to some degree through cultivation. Still, they also increase soil loss rates by disrupting the soil parameters (Imajjane & Belfoul, 2020). Bera (2017) found that dense forest and densely rubber plantations had lower CP factor values (0.008–0.02), whereas wasteland and barren land had higher values (0.34–0.6). The present examination results with outcomes of other studies indicate that vegetative cover highly reduces soil erosion in the Kashmir region and different nations elsewhere (Ebabu et al., 2019).

P Factor

P factor values can be reduced by various conservation activities like contouring, terracing, alternate cropping, strip cropping, creation of bunds etc. (Barman et al., 2020). The higher values were given to land-use practices with limited or no conservation practices, whereas lower values were assigned to areas with no erosion. Effective conservation measures signify lower P values (Bhat et al., 2017). In South eastern Nigeria, Amah et al. (2020) observed that P values went from 0.56 to 1.0, with larger values indicating the absence of any conservation technique, implying that erosion is at its peak due to the lack of any management

practice. The outcomes demonstrate that snow-covered areas, waterbody and wastelands with no support practices had a higher *P*-value of 1. In contrast, built-up areas with minimal soil erosion had a value of 0. Due to the presence of conservation support practice (terracing) which protected the soil from erosion, the TOF practices and agriculture were assigned a value of 0.3 and 0.2, respectively. The forest, forest scrub, grassland and wetland were set values close to 1 due to the absence of conservation practices, but the presence of vegetative cover in these land uses. The outcomes of the present study authenticate with the findings of Srinivasan et al. (2019) for Odisha, India (0–1) and Das et al. (2021) for the Noghoh micro watershed of Ri-Bhoi district of Meghalaya (0.6–1). Thus, the presence of anti-erosion practices aids in the reduction of soil disintegration in regions of steeper slants where erosion rates are otherwise comparatively extreme (Imajjane & Belfoul, 2020).

Soil Erosion Vulnerability

Mapping soil erosion vulnerability is valuable for the rapid identification and pre-selection of hotspot areas prone to erosion for the district management planning. In the present study, in the severely vulnerable class, the maximum values fell between 120 and 1500 t/ha; hence these two values were used to calculate mean soil loss for this category. Using actual values (120–6100) t/ha, for calculating the mean value would have unnecessarily increased the mean value and affected the statistical analysis. The maximum (137,165.30 ha) area was under less vulnerable class (0–30 t/ha/yr) due to the higher percentage of forest (33.96%). The severely vulnerable group associated with a high soil loss rates was scattered in the vulnerability map. Barman et al. (2020) tracked down that 70.21% of a watershed in Mizoram (India) was under slight/very low risk (< 20 Mg/ha/yr), 6.53% under very high risk (20–40 Mg/ha/yr) and 9.92% under very severe risk (more than 80 Mg/ha/yr). In another study carried out by Sotiropoulou et al. (2011), 58.2% of the Komotini, Greece, was found to be under no erosion hazard, 16.4% minimum to moderate, 9.1% moderate to severe, 5.1% severe to very severe and 11.1% under highly severe erosion risk. The present study reasoned that the areas with a predominance of agriculture, wasteland, grassland and glacier had a greater vulnerability. The primary driver for severe erosion could be high erodibility values, steep slopes and improper land management practices like deforestation, intensive cultivation and poor vegetation. Das and Patgiri (2020) found 77.45 per cent of the Palla river basin in Assam to be in the least risk category, 4.56 per cent to be in the low risk category, 5.31 per cent to be in the moderate risk category, 7.69 per cent to be in the high risk category, and 4.99 per cent to be in the very high risk category. From the outcomes of the current investigation, it is clear that some

areas of the study region are severely vulnerable to erosion, requiring the utmost attention to prevent these areas from reaching a point where it would be difficult to revert the repercussions of soil erosion.

Validation of Soil Erosion Vulnerability

The field validity of the generated soil vulnerability model is a significant prerequisite in the vulnerability modeling approach. The validation of the model was assessed by approving the soil erosion vulnerability with ground-truthing, which involves investigating areas (sample locations) of the generated soil vulnerability map cross-checked with high resolution google earth images/ ground-truthing. A total of 30 high erosion points were picked randomly (15 from the severe vulnerability category and 15 from the extreme vulnerability category). The selected points were then located on google earth to record the geographic directions. Some of the physically accessible locations were subsequently visited to check and verify the occurrence of soil erosion in these areas. However, for inaccessible high erosion locations, the help of google earth was taken to locate the areas for physical appearance and land use to verify deciphered outcomes. The validation points from the field largely matched (> 95%) their respective vulnerability category. The results uncovered that the severely and highly vulnerable sample points were under wasteland and snow land-use practices with higher elevation among the chosen locations, thus demanding additional consideration to prevent these areas from deteriorating. The validation of soil erosion vulnerability revealed that the RUSLE model could explain the soil disintegration hazard occurrence in an ideal manner.

Conclusion

Soil disintegration models are constructive for surveying the likely impacts of environment driven land-cover changes on soil loss rates and characterizing the need for robust and reasonable land-use planning. While often easy and simple to decipher, empirical soil disintegration modeling needs comparatively limited assets. It can be carried out with promptly accessible elements to recognize the regions subject to high soil loss. The present study explains the use of RUSLE in conjunction with GIS for soil hazard mapping, its spatial variation, and the prioritization of hotspot areas subjected to soil erosion. The outcomes reasoned that the regions with a predominance of agriculture, wasteland, forest scrub and glacier had a greater vulnerability. High erodibility values, steep slopes, and improper land management could be the primary driver of severe erosion. The outcomes report soil disintegration from the agricultural lands due to inappropriate land conservation exercises like deforestation, intensive

cultivation and poor vegetation. The hotspot areas identified in the present study are under expanding level of soil loss, necessitating purposeful endeavors to reduce soil disintegration and its related issues. The present study's findings will aid in framing management strategies by providing baseline data to strategy makers to oversee soil erosion hazards most proficiently, optimize productivity and contribute to farmers' enhanced performance income.

Acknowledgements The authors acknowledge the support received from the field staff of the Division of Natural Resource Management, Faculty of Forestry SKUAST-K in carrying out the field activities regarding preliminary survey, collection of soil samples and ground truth points.

Author Contributions Each author contributed to the work under different capacities. SZ and AAW conceptualized the design and drafted the manuscript. SZ, AAG, MAI and SM collected and compiled the field data. SZ, AAW, THM and PKJ carried out the data analysis. All authors contributed in reviewing the manuscript.

Funding We thank the Department of Science and Technology, Government of India, for providing financial support to the Author 1 (SZ) in carrying out this study under INSPIRE Fellowship no. DST/INSPIRE Fellowship/2018/IF180413. We also thank EACEA to enable us to use the equipment purchased by the Author 2 (AAW) under Erasmus + funded URGENT project (No: 619050-EPP-1-2020-1-DE-EPPKA2-CBHE-JP).

Declarations

Conflict of interest The authors declared that they have no conflict of interest.

References

- Alewell, C., Borrelli, P., Meusburger, K., & Panagos, P. (2019). Using the USLE: Chances, challenges and limitations of soil erosion modeling. *International Soil and Water Conservation Research*, 7(3), 203–225. <https://doi.org/10.1016/j.iswcr.2019.05.004>.
- Alexakis, D. D., Hadjimitsis, D. G., & Agapiou, A. (2013). Integrated use of remote sensing, GIS and precipitation data for the assessment of soil erosion rate in the catchment area of Yialias in Cyprus. *Atmospheric Research*, 131, 108–124. <https://doi.org/10.1016/j.atmosres.2013.02.013>.
- Amah, J. I., Aghamelu, O. P., Omonona, O. V., & Onwe, I. M. (2020). A Study of the dynamics of soil erosion using RUSLE modelling and geospatial tool in Edda-Afikpo Mesas, south eastern Nigeria. *Pakistan Journal of Geology*, 4(2), 56–71. <https://doi.org/10.2478/pjg-2020-0007>.
- Amsalu, A., Stroosnijder, L., & Graaf, J. (2007). Long-term dynamics in land resource use and the driving forces in the Beressa watershed, highlands of Ethiopia. *Journal of Environmental Management*, 83(4), 448–459. <https://doi.org/10.1016/j.jenvman.2006.04.010>.
- Anonymous. (2011). Directorate of economics and statistics. District statistics and evaluation office, Ganderbal, Jammu and Kashmir.
- Anonymous. (2014). Climate of Jammu and Kashmir. climatological publication section, Office of Additional Director General of Meteorology (Research), Pune.
- Arekhi, S., Niazi, Y., & Kalteh, A. M. (2012). Soil erosion and sediment yield modeling using RS and GIS techniques: A case study

- Iran. *Arabian Journal of Geosciences*, 5(2), 285–296. <https://doi.org/10.1007/s12517-010-0220-4>.
- Babu, R., Dhyani, B. L., & Kumar, N. (2004). Assessment of erodibility status and refined Iso-Erodent Map of India. *Journal of Soil and Water Conservation*, 32(2), 171–177.
- Bahrami, H. A., Vaghei, H. G., Vaghei, B. G., Tahmasbipour, N., & Tabari, T. F. A. (2005). New method for determining the soil erodibility factor based on fuzz systems. *Journal of Agricultural Science and Technology*, 17, 115–123.
- Barman, B. K., Rao, K. S., Sonowal, K., Zohmingliani, Prasad, N. S. R., & Sahoo, U. K. (2020). Soil erosion assessment using revised universal soil loss equation model and geo-spatial technology: A case study of upper Tuirial river basin, Mizoram India. *AIMS Geosciences*, 6(4), 525–544. <https://doi.org/10.3934/geosci.2020030>.
- Belayneh, M., Yirgu, T., & Tsegaye, D. (2019). Potential soil erosion estimation and area prioritization for better conservation planning in Gumara watershed using RUSLE and GIS techniques. *Environmental Systems Research*. <https://doi.org/10.1186/s40068-019-0149-x>.
- Bera, A. (2017). Estimation of Soil loss by USLE Model using GIS and Remote Sensing techniques: A case study of Muhuri River Basin, Tripura, India. *Eurasian J Soil Sci*, 6(3), 206–215. <https://doi.org/10.18393/ejss.288350>.
- Beskow, S., Mello, C. R., & Norton, L. D. (2009). Soil erosion prediction in the Grande river basin Brazil Using Distributed Modeling. *Catena*, 79(1), 49–59. <https://doi.org/10.1016/j.catena.2009.05.010>.
- Bhat, S. A., Hamid, I., Dar, M. D., Rasool, D., Pandit, B. A., & Khan, S. (2017). Soil erosion modeling using RUSLE & GIS on micro watershed of J&K. *Journal of Pharmacognosy and Phytochemistry*, 6(5), 838–842.
- Borrelli, P., Robinson, D. A., Fleischer, L. R., Lugato, E., Ballabio, C., Alewell, C., Meusburger, K., Modugno, S., Schütt, B., Ferro, V., Bagarello, V., Van, O. K., Montanarella, L., & Panagos, P. (2013). An assessment of the global impact of 21st century land use change on soil erosion. *Nature Communications*. <https://doi.org/10.1038/s41467-017-02142-7>.
- Bouhadeb, C. E., Menani, M. R., Bouguerra, H., & Derdous, O. (2018). Assessing soil loss using GIS based RUSLE methodology. Case of the Bou Namoussa watershed—Northeast of Algeria. *J Water Land Dev*, 36, 27–35. <https://doi.org/10.2478/jwld-2018-0003>.
- Brady, N. C., & Weil, R. R. (2000). *Elements of the Nature and Properties of soils*. Upper Saddle River (NJ), USA: Prentice Hall.
- Brady, N. C., & Weil, R. C. (2012). *The nature and properties of soils*. Pearson education, New Delhi.
- Chadli, K. (2016). Estimation of soil loss using RUSLE model for Sebou Watershed (Morocco). *Modeling Earth Systems and Environment*, 2(2), 1–10. <https://doi.org/10.1007/s40808-016-0105-y>.
- Choudhury, M. K., & Nayak, T. (2003). Estimation of Soil Erosion in Sagar Lake Catchment of Central India, Proceedings of the International Conference on Water and Environment, Bhopal, India. pp. 387–392.
- Dar, R. A., Romshoo, S. A., Chandra, R., & Ahmad, I. (2014). Tectono-geomorphic study of the Karewa Basin of Kashmir Valley. *Journal of Asian Earth Sciences*, 92, 143–156. <https://doi.org/10.1016/j.jseae.2014.06.018>.
- Das, M., & Patgiri, M. (2020). Soil loss estimation using revised universal soil loss equation (RUSLE) model for Palla river basin Assam. *International Journal of Advanced Science and Technology*, 29(4), 4369–4377.
- Das, D. D. C., Bali, Y. P., & Kaul, R. N. (1981). Soil conservation in multipurpose river valley catchments. Problems, programme approaches and effectiveness. *Journal of Soil and Water Conservation*, 9, 5–26.
- Das, B., Bordolo, R. S., Thungon, L. T., Paul, A., Pandey, P. K., Mishra, M., & Tripathi, O. P. (2020). An integrated approach of GIS, RUSLE and AHP to model soil erosion in West Kameng watershed Arunachal Pradesh. *Journal of Earth System Science*, 129(94), 1–18.
- Das, S., Deb, P., Bora, P. K., & Katre, P. (2021). Comparison of RUSLE and MMF Soil Loss Models and Evaluation of Catchment Scale Best Management Practices for a Mountainous Watershed in India. *Sustainability*, 13(1), 232. <https://doi.org/10.3390/su13010232>.
- Dimotta, A. (2019). Soil erosion interdisciplinary overview: Modeling approaches, ecosystem services assessment and soil quality Restoration. Applications and analysis in the Basilicata region (Italy). Ph.D. Thesis.
- Ebabu, K., Tsunekawa, A., Haregeweyn, N., Adgo, E., Meshesha, D. T., Aklog, D., Masunaga, T., Tsubo, M., Sultan, D., Fenta, A. A., & Yibeltal, M. (2019). Effects of land use and sustainable land management practices on runoff and soil loss in the Upper Blue Nile basin, Ethiopia. *Science of the Total Environment*, 648, 1462–1475. <https://doi.org/10.1016/j.scitotenv.2018.08.273>.
- Erkossa, T., Wudneh, A., Desalegn, B., & Taye, G. (2015). Linking soil erosion to on-site financial cost: Lessons from watersheds in the Blue Nile basin. *Solid Earth*, 6, 765–774. <https://doi.org/10.5194/se-6-765-2015>.
- Evans, R. (1980). *Mechanics of water erosion and their spatial and temporal controls: an empirical viewpoint*. Soil Erosion, Wiley, New York, USA.
- FAO, ITPS. (2015). Status of the World's Soil Resources (SWSR)-Main Report, Food and Agriculture Organization of the United Nations and Intergovernmental Technical Panel on Soils, Rome, Italy.
- Farhan, Y., & Nawaiseh, S. (2015). Spatial assessment of soil erosion risk using RUSLE and GIS techniques. *Environment and Earth Science*, 74(6), 4649–4669. <https://doi.org/10.1007/s12665-015-4430-7>.
- Farhan, Y., Zreقات, D., & Nawaysa, S. (2014). Assessing the influence of physical factors on spatial soil erosion risk in northern Jordan. *American Journal of Science*, 10, 29–39.
- Fenta, A. A., Yasuda, H., Shimizu, K., Haregeweyn, N., & Negussie, A. (2016). Dynamics of soil erosion as influenced by watershed management practices: A case study of the Agula watershed in the semi-arid highlands of Northern Ethiopia. *Environmental Management*, 58(5), 889–905. <https://doi.org/10.1007/s00267-016-0757-4>.
- Foster, G., Yoder, D., Weesies, G., McCool, D., McGregor, K., & Binger, K. (2003). *User's guide revised—universal soil loss equation version 2 (RUSLE 2)*. USDA—Agricultural Research Service Washington. DC Google Scholar.
- Ganai, I. H. (2014). Estimation of soil erosion for Himalayan micro-watershed using GIS technique. Ph. D. Thesis. Sher-e-Kashmir University of Agricultural Sciences and Technology, Kashmir, India.
- Ganasri, B. P., & Ramesh, H. (2015). Assessment of soil erosion by RUSLE model using remote sensing and GIS—A case study of Nethravathi Basin. *Geoscience Frontiers*, 30, 1–9. <https://doi.org/10.1016/j.gsf.2015.10.007>.
- Gianinetto, M., Aiello, M., Polinelli, F., Frassy, F., Rulli, M. C., Ravazzani, G., Bocchiola, D., Chiarelli, D. D., Soncini, A., & Vezzoli, R. (2019). D-RUSLE: A dynamic model to estimate potential soil erosion with satellite time series in the Italian Alps. *European Journal of Remote Sensing*, 52(4), 34–53. <https://doi.org/10.1080/22797254.2019.1669491>.
- Govindarajan, S. V. (1978). *Studies on soils of India*. Vikas Publishing House.
- Goy, P. N. (2015). GIS-based soil erosion modeling and sediment yield of the N'djili river basin, Democratic Republic of Congo. M. Sc.

- Thesis. Department of Civil and Environmental Engineering Colorado State University.
- Gupta, S., & Kumar, S. (2017). Simulating climate change impact on soil erosion using RUSLE model—A case study in a watershed of mid-Himalayan landscape. *Journal of Earth System Science*. <https://doi.org/10.1007/s12040-017-0823-1>.
- Haile, G. W., & Fetene, M. (2012). Assessment of soil erosion hazard in Kilie catchment, East Shoa, Ethiopia. *Land Degradation and Development*, 23, 293–306. <https://doi.org/10.1002/ldr.1082>.
- Haregeweyn, N., Tsunekawa, A., Poesen, J., Tsubo, M., Meshesha, D. T., Fenta, A. A., Nyssen, J., & Adgo, E. (2017). Comprehensive assessment of soil erosion risk for better land use planning in river basins: Case study of Upper Blue Nile River. *Science of the Total Environment*, 574, 95–108. <https://doi.org/10.1016/j.scitotenv.2016.09.019>.
- Imajjane, L. B., & Belfoul, M. A. (2020). Soil loss assessment in western high Atlas of Morocco: Beni Mohand watershed study case. *Applied and Environmental Soil Science*. <https://doi.org/10.1155/2020/6384176>
- Islam, Md. R., Imran, H. M., Islam, Md. R., & Saha, G. C. (2024). A RUSLE-based comprehensive strategy to assess soil erosion in a riverine country, Bangladesh. *Environmental Earth Sciences*, 83, <https://doi.org/10.1007/s12665-024-11455-y>.
- Jazouli, A. E., Barakat, A., Ghafiri, A., Moutaki, S. E., Ettaqy, A., & Khellouk, R. (2017). Soil erosion modeled with USLE, GIS, and remote sensing: A case study of Ikkour watershed in Middle Atlas (Morocco). *Geoscience Letter*, 4, 25. <https://doi.org/10.1186/s40562-017-0091-6>.
- Kenneth, G., George, R., Foster, G. A., Weesies, D. K., & McCool Yoder, D. C. (1997). *Predicting soil erosion by water: A guide to conservation planning with the Revised Universal Soil Loss Equation (RUSLE)* (703rd ed.). United States Department of Agriculture.
- Kidane, M., Bezie, A., Kesete, N., & Tolessa, T. (2019). The impact of land use and land cover (LULC) dynamics on soil erosion and sediment yield in Ethiopia. *Heliyon*. <https://doi.org/10.1016/j.heliyon.2019.e02981>.
- Kumar, S., & Kushwaha, S. P. S. (2013). Modelling soil erosion risk based on RUSLE-3D using GIS in a Shivalik sub-watershed. *Journal of Earth System Science*, 122(2), 389–398. <https://doi.org/10.1007/s12040-013-0276-0>.
- Labriere, N., Locatelli, B., Laumonier, Y., Freycon, V., & Bernoux, M. (2015). Soil erosion in the humid tropics: A systematic quantitative review. *Agriculture, Ecosystems & Environment*, 203, 127–139. <https://doi.org/10.1016/j.agee.2015.01.027>.
- Mandal, D., & Sharda, V. N. (2011). Appraisal of soil erosion risk in the eastern Himalayan region of India for soil conservation planning. *Land Degradation and Development*, 24, 430–437.
- Manjulavani, K., Prathyusha, B., & Ramesh, M. (2016). Soil erosion and sediment yield modeling using remote sensing and GIS techniques. *International Journal of Applied Management*, 2(10), 59–63.
- Maqsoom, A., Aslam, B., Hassan, U., Kazmi, Z. A., Sodangi, M., Tufail, R. F., & Farooq, D. (2020). Geospatial assessment of soil erosion intensity and sediment yield using the revised universal soil loss equation (RUSLE) model. *International Journal of Geoinformatics*, 9, 356–369. <https://doi.org/10.3390/ijgi9060356>.
- McCool, D. K., Papendick, R. I., & Hammel, J. E. (1995). Surface residue management. In R. I. Papendick (Ed.), *Crop residue management to reduce erosion and improve soil quality*. Eds. R.I. Papendick, W.C. Moldenhauer. USDA: Conservation Report.
- Meusburger, K., Steel, A., Panagos, P., Montanarella, L., & Alewell, C. (2012). Spatial and temporal variability of rainfall erosivity factor for Switzerland. *Hydrology and Earth System Sciences*, 16, 167–177. <https://doi.org/10.5194/hess-16-167-2012>.
- Ministry of Agriculture and Farmers Welfare. (2020). Conversion of Barren Land into Arable Land [Press release]. <https://pib.gov.in/PressReleaseDetailm.aspx?PRID=1607339>.
- Olaniya, M., Bora, P. K., Das, S., & Chanu, P. K. (2020). Soil erodibility indices under different land uses in Ri-Bhoi district of Meghalaya (India). *Scientific Reports*, 10, 14986. <https://doi.org/10.1038/s41598-020-72070-y>.
- Ostovari, Y., Dashtaki, S. G., Bahrami, H. A., Naderi, M., & Dematte, J. A. M. (2017). Soil loss estimation using RUSLE model, GIS and remote sensing techniques: A case study from the Dembercha Watershed Northwestern Ethiopia. *Geoderma*, 11(2), 28–36. <https://doi.org/10.1016/j.geoder.2017.06.003>.
- Panagos, P., Borrelli, P., & Meusburger, K. (2015). A new European slope length and steepness factor (LS-Factor) for modeling soil erosion by water. *Geosciences*, 5(2), 117–126. <https://doi.org/10.3390/geosciences5020117>.
- Pandey, A., Chowdary, V. M., & Mal, B. C. (2017). Identification of critical erosion prone areas in the small agricultural watershed using USLE, GIS and remote sensing. *Water Resource Management*, 21, 729–746. <https://doi.org/10.1007/s11269-006-9061-z>.
- Panditharathne, D. L. D., Abeysingha, I. N. S., Nirmanee, K. G. S., & Mallawatantri, A. (2019). Application of revised universal soil loss equation (RUSLE) model to assess soil erosion in Kalu Ganga River basin in Sri Lanka. *Applied and Environmental Soil Science*. <https://doi.org/10.1155/2019/4037379>.
- Prasannakumar, V., Shiny, R., Geetha, N., & Vijith, H. (2011). Spatial prediction of soil erosion risk by remote sensing, GIS and RUSLE approach: A case study of Siruvani River Watershed in Attapady Valley, Kerala, India. *Environment and Earth Science*, 46, 965–972. <https://doi.org/10.1007/s12665-011-0913-3>.
- Rawat, K. S., Mishra, A. K., & Bhattacharyya, R. (2016). Soil erosion risk assessment and spatial mapping using LANDSAT-7 ETM þ, RUSLE, and GIS—a case study. *Arabian Journal of Geosciences*. <https://doi.org/10.1007/s12517-015-2157-0>.
- Raza, M., Ahmad, A., & Mohammad, A. (1978). *The valley of Kashmir: A geographical Interpretation*. Vikas Publishing House.
- Saroha, J. (2017). Soil erosion: Causes extent and management in India. *International journal of creative research thoughts*, 5(4), 1321–1330.
- Sharma, J. C., & Chaudhary, S. K. (2007). Land use, nutrient indexing and soil fertility mapping of Mandhala watershed in Shivalik foot hills of Himachal Pradesh—A GIS approach. *Agropedology*, 17(1), 41–49.
- Sharma, J., & XuSharma, G. (2007). Traditional agroforestry in the eastern Himalayan region: Land management system supporting ecosystem services. *Tropical Ecology*, 48(2), 189–200.
- Shoumik, B. A. A.; Khan, Md. Z. and Islam, Md. S. (2023). Soil erosion estimation by RUSLE model using GIS and remote sensing techniques: A case study of the tertiary hilly regions in Bangladesh from 2017 to 2021. *Environmental Monitoring and Assessment*. 195. <https://doi.org/10.1007/s10661-023-11699-4>.
- Singh, G., & Panda, R. K. (2017). Grid-cell based assessment of soil erosion potential for identification of critical erosion prone areas using USLE, GIS and remote sensing: A case study in the Kapgari watershed India. *International Soil and Water Conservation Research*, 5(3), 202–211. <https://doi.org/10.1016/j.iswcr.2017.05.006>.
- Singh, G., Babu, R., Narain, P., Bhusan, L. S., & Abrol, I. P. (1992). Soil erosion rates in India. *Journal of Soil and Water Conservation*, 47(1), 97–99.
- Sotiropoulou, A. M., Alexandridis, T., Bilas, G., Karapetsas, N., Tzelou, A., Silleos, N., & Misopolinos, N. (2011). A user friendly GIS model for the estimation of erosion risk in agricultural land using the USLE. In: M. Salampasis, A. Matapoulos (Eds.): Proceedings of the International Conference on Information and

- Communication Technologies for Sustainable Agri-production and Environment (HAICTA 2011), Skiathos.
- Srinivasan, R., Singh, S. K., Nayak, D., Hegde, R., & Ramesh, M. (2019). Estimation of soil loss by USLE Model using remote sensing and GIS techniques—A case study of coastal Odisha, India. *Eurasian Journal of Soil Science*, 8(4), 321–328. <https://doi.org/10.18393/ejss.598120>.
- Tamiru, H., & Wagari, M. (2021). RUSLE model based Annual Soil Loss Quantification for soil erosion protection in Fincha Catchment, Abay River Basin, Ethiopia. *Preprints*. <https://doi.org/10.20944/preprints202102.0526.v1>.
- Thapa, P. (2020). Spatial estimation of soil erosion using RUSLE modeling: A case study of Dolakha district Nepal. *Environmental System Research*. <https://doi.org/10.1186/s40068-020-00177-2>.
- Uddin, K., Matin, M. A., & Maharjan, S. (2018). Assessment of land cover change and its impact on changes in soil erosion risk in Nepal. *Sustainability*, 10(12), 4715–4726. <https://doi.org/10.3390/su10124715>
- Wang, J., Qian, H., Zhou, P., & Gong, Q. (2019). Test of the RUSLE and key influencing factors using GIS and probability methods: A case study in Nanling national nature reserve South China. *Advanced Civil Engineering*. 7129639, <https://doi.org/10.1155/2019/7129639>.
- Wani, A. A., Joshi, P. K., Singh, O., Kumar, R., & Rawat, V. R. S. (2017). Forest biomass carbon dynamics (1980–2009) in Western Himalaya in the context of REDD+ policy. *Environment and Earth Science*, 76, 573. <https://doi.org/10.1007/s12665-017-3903-3>.
- Wani, A. A., Bhat, A. F., Gatoo, A. A., Zahoor, S., Mehraj, B., Najam, N., Wani, Q. S., Islam, M. A., Murtaza, S., Dervash, M., & Joshi, P. K. (2021). Assessing relationship of forest biophysical factors with NDVI for carbon management in key coniferous strata of temperate Himalayas. *Mitigation and Adaptation Strategies for Global Change*, 26(1), 1–22. <https://doi.org/10.1007/s11027-021-09937-6>.
- Wischmeier, W. H., & Smith, D. D. (1965). Prediction rainfall erosion losses from cropland east of the rocky mountains: A guide for selection of practices for soil and water conservation. *Agricultural Handbook*, 282, 48.
- Wischmeier, W. H., & Smith, D. D. (1978). *Predicting rainfall erosion losses: guide to conservation planning* (537th ed.). USDA Agriculture Handbook 537. U.S. Government Printing Office, Washington, DC.
- Wischmeier, W. H., Johnson, C. B., & Cross, B. V. (1971). Soil erodibility nomograph for farmland and construction sites. *Journal of Soil and Water Conservation*, 26, 189–193.
- Yesuph, A. Y., & Dagne, A. B. (2019). Soil erosion mapping and severity analysis based on RUSLE model and local perception in the Beshillo Catchment of the Blue Nile Basin, Ethiopia. *Environmental Systems Research*, 8(1), 1–21. <https://doi.org/10.1186/s40068-019-0145-1>.
- Zhang, H., Yang, Q., Li, R., Liu, Q., Moore, D., He, P., Ritsema, C. J., & Geissen, V. (2013). Extension of a GIS procedure for calculating the RUSLE equation LS factor. *Computers & Geosciences*, 52, 177–188. <https://doi.org/10.1016/j.cageo.2012.09.027>.
- Zonunsanga, R. (2016). Estimation of Soil loss in Teirei watershed of Mizoram by using the USLE Model. *J Sci Tech*, 4, 43–47.

Publisher's Note Springer Nature remains neutral with regard to jurisdictional claims in published maps and institutional affiliations.

Springer Nature or its licensor (e.g. a society or other partner) holds exclusive rights to this article under a publishing agreement with the author(s) or other rightsholder(s); author self-archiving of the accepted manuscript version of this article is solely governed by the terms of such publishing agreement and applicable law.